Theoretical spectroscopic studies of potential energy curves and Fortran parabola for beryllium oxide molecule

Marwa Waleed Mahmod[1], Dhia Hamde Al-Amedy[1], Zeyad Adnan Saleh[2]

[1]Department of Physics, College of Science for Women, University of Baghdad

[2]Department of Physics, College of Science, AL-Mustansriyah University

E-mail: marwa_88w@yahoo.com

Abstract

Theoretical spectroscopic studies of beryllium oxide has been carried out, potential energy curves for ground states $X^1\Sigma^+$ and exited states $A^1\Pi$, $B^1\Sigma^+$ by using two functions Morse and Varshni compared with experimental results. The potentials of this molecule are agreement with experimental results. The Fortrat Parabola corresponding to $R(J), Q(J)$ and $P(J)$ branches were determined in the range $1 \leq J \leq 20$ for the (0-0) band. It was found that for electronic transition $A1\Pi - X^1\Sigma^+$ the bands head lies in R branche of Fortrat parabola and the bands degraded towards red region. For electronic transition $B^1\Sigma^+$ - $A^1\Pi$ Fortart parabola appeared the bands head lies in P branche and the bands degraded toward violet region.

دراسة نظرية طيفية لمنحنيات طاقة الجهد ومنحني فورتران لجزيئة اوكسيد البريليوم

مروة وليد محمود1، ضياء حمدي العميدي1، زياد عدنان صالح2

1قسم الفيزياء، كلية العلوم للبنات، جامعة بغداد

2قسم الفيزياء، كلية العلوم، الجامعة المستنصرية

الخلاصة

اجريت دراسة نظرية طيفية تضمنت حساب منحني الجهد لجزيئة اوكسيد البريليوم BeO للحالة الارضية $X^1\Sigma^+$ والحالتين المتهيجتين $A^1\Pi$, $B^1\Sigma^+$ بإستخدام دالتي Morse, Varshni ولوحظ ان النتائج المحسوبة نظريا تتوافق مع النتائج العملية فضلا عن حساب منحني فورترات للفروع $R(J)$, $P(J),Q(J)$ للحزمة (0-0) في مدى الاعداد الكمية الدورانية $1 \leq J \leq 20$ تتجه هذه الفروع للإنتقال الالكتروني $A^1\Pi - X^1\Sigma^+$ بإتجاه المنطقة تحت الحمراء ويظهر رئسا الحزمة R,Q اما عند الإنتقال الالكتروني $B^1\Sigma^+$ - $A^1\Pi$ تتجه الفروع بإتجاه المنطقة فوق البنفسجية ويظهر رئسا الحزمة عند P,Q.

Introduction

Beryllium oxide is a white crystalline oxide can be prepared by calcining (roasting) beryllium carbonate, dehydrating beryllium hydroxide or igniting the metal. Beryllium oxide is used in many high-performance semiconductor parts for applications such as radio equipment because it has good thermal conductivity while also being a good electrical insulator. It is also used as a structural ceramic for high-performance microwave devices, vacuum tubes, magnetrons, and gas lasers [1]. Much interest is being focused on the theoretical aspects of the Beryllium Oxide molecule which had astrophysical importance like other oxide of alkaline

earths [2]. Lagerqvist (1948) measured the potential energy curve and the dissocation energy for ground state, first excited state and second excited state for beryllium oxide [3]. Herzberg (1950) calculated the Fortrat parbola for electronic transition of AIH and CN molecules for system [4]. Conkic et al. (1978) calculated the Fortrat parabola of $^{12}C^{16}O^+$ molecule for (0-0) band [5]. Narasimhamurthy and Rajamanickam (1981) calculated the potential energy curve for AIH and CaH molecules [6]. Tawde and Tulasigeri (1986) studied Franck – Condon factors and electronic transition moment for $B^1\Sigma$-X $^1\Sigma$ band system of BeO molecule [2]. Lto et al (1992) calculated the wave numbers for P,Q and R branches of $B^2\Sigma$-$X^2\Sigma$ system of CN molecule [7]. Hirao et al. (2000) calculated the Fortart parabola of $A^2\Pi$ -$X^2\Sigma$ for MgBr molecule (0-0) band [8]. Daily et al. (2002) calculated the transition probabilities in the $B^1\Sigma$ -$X^1\Sigma$ and $B^1\Sigma$-$A^1\Pi$ electronic system of MgO molecule [9]. Groh et al (2009) studied optical properties such as the dynamic dielectric function, reflectance, and energy-loss function of BeO molecule [10]. AL-Amiedy et al (2011) studied the Fortrat parabola of LiH molecule [11]. Shayesth et al (2013) calculated the wave number P,Q and R of the (0-0) band of $B^2\Sigma$-$A^2\Pi$ and $A^2\Pi$-$X^2\Sigma$ system of CaH molecule [12].

Theory

The electronic state is represented, usually by a potential energy curve refers to apposition and values of energy for this state depending upon the internuclear distance. There are many functions for potential energy curve of diatomic molecule and concern the Morse potential is the simplest representative of the potential between two nuclei in which dissociation is possible. The form of the Morse potential, which rewrite the potential as [4].

$$Vm = De\left[1 - e^{-\beta(r-re)}\right]^2 \qquad (1)$$

D_e dissociation energy and β parameters of Morse potential function are to be determined by these equations. r, r_e are the distance and the equilibrium distance between two atoms respectively.

$$\beta = [8\pi^2\,\mu\,\omega_e\,x_e c/h]^{1/2} \qquad (2)$$

ω_e : harmonic vibrational constant

x_e: unharmonic vibrational constant

c: velocity of light

h: planck constant

$$D_e = \frac{\omega_e^2}{4\,\omega_e\,x_e} \ , \qquad (3)$$

The other function of potential is Varshini function which is different from Morse function term r/r_e so the function had written as [13]

$$V_m = De\left[1 - \frac{r}{r_e}e^{-\beta(r-re)}\right]^2 \qquad (4)$$

The absorption or emission of electromagnetic radiation in visible and UV regions results from the transition happens between the electronic energy levels of the molecules. The nature of the rotational fine structure of electronic transition is largely dependent up on the levels or states involved in the transition. If the transition had happens from an excited electronic state to ground state the effect of rotation and vibration had been taken , then the spectral transition for the molecule will be given by the relationship [14].

$$\Delta E = \Delta T_e + \Delta G_v + \Delta F_J , \qquad (5)$$

$$E' - E'' = T_e' - T_e'' + G_v' - G_v'' + F_J' - F_J'', \qquad (6)$$

where ΔT_e represent the energy difference between electronic energy levels, ΔG_v represent the difference between the vibrational energy levels and ΔF_J represent the difference between the rotational energy levels. The vibration energy given by the relationship [15].

$$G_v = \omega_e\left[v + \frac{1}{2}\right] - \omega_e\,x_e\left[v + \frac{1}{2}\right]^2 , \qquad (7)$$

where v is vibrational quantum number,

$$Vm = De\left[1 - e^{-\beta(r-re)}\right]^2, \qquad (1)$$

The rotational energy given by the relationship

$$F_J = B_v \, J(J + 1) \qquad (8)$$

where J is rotational quantum number

$$B_v = B_e - \alpha_e \left[v + \tfrac{1}{2}\right], \qquad (9)$$

Eq. (9) represent the relation of rotational constant and vibrational quantum number (v), where B_e is the rotational constant corresponding to the equilibrium bond distance α_e is the vibration - rotation interaction constant. Fortrat parabola could be found from the relation between

R(J),P(J), Q(J) and m using the following equations [16]

$$R(J),P(J) = v_0 + (B_v + B_v)\, m + (B_v - B_v)\, m^2 \qquad (10)$$

$$Q(J) = v_0 + (B_v' - B_v'')m + (B_v' - B_v'')m^2 \qquad (11)$$

For P(J) branch at m= -J, R(J) at m= J+1 and Q(J) at m= J, v_0 is the frequency of the band origin could be given by this equation

$$v_0 = \Delta T_e + \Delta G_v , \qquad (12)$$

Results and Discussion

The spectroscopic constants of beryllium oxide molecule are given in Table1.

Table. 1: The diatomic constants for the ground states and the excited state of BeO used in calculation.

State	$X^1\Sigma^+$	$A^1\Pi$	$B^1\Sigma^+$
T_e cm^{-1}	0	9405.61	2153.94l
ω_e cm^{-1}	1487.32	1144.24	1370.82
$\omega_e\, x_e$cm^{-1}	11.830	8.415	7.746
B_e	1.6510	1.3661	1.5758
α_e	0.0190	0.01628	0.0154
r_e cm	1.3309×10^{-8}	1.4631×10^{-8}	1.3623×10^{-8}

It was found that from Figs. (1-3) and Tables (2-4) the theoretical results for Morse and Varshini potential energy curves agree with experimental results.
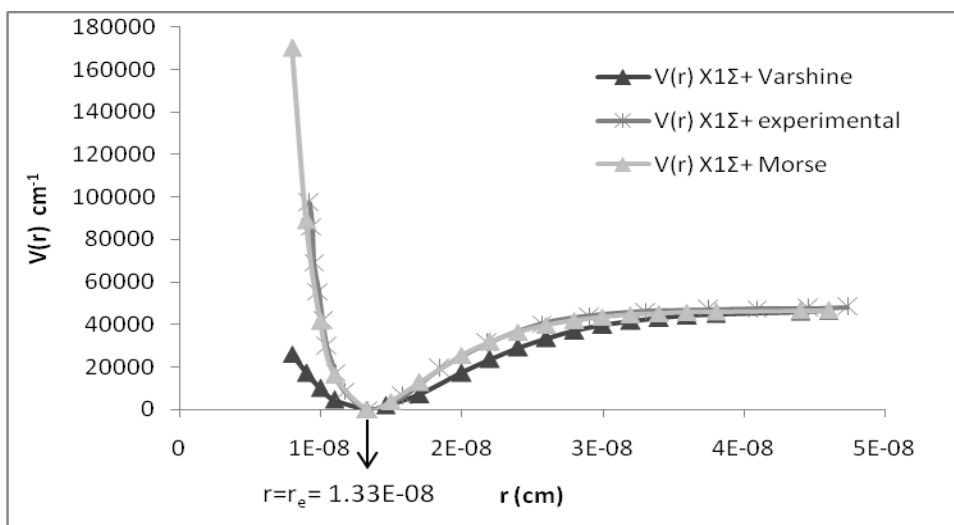

Fig.1: Theoretical potential calculated by Morse and Varshine function compare with the experimental curves for ground state $X^1\Sigma^+$.

Table 2: Theorttical and experimental Values of potential energy for ground state $X^1\Sigma^+$ of BeO molecule.

r (cm)	V(r) $X^1\Sigma^+$ (cm^{-1}) Morse	V(r) $X^1\Sigma^+$ (cm^{-1}) Varshine	r (cm) [3]	V(r) $X^1\Sigma^+$ (cm^{-1}) experimental [3]
8E-09	170338.11	26181.58	9.23E-09	97306.5
9E-09	88897.05	17316.91	9.38E-09	86161
1E-08	41804.01	9968.88	9.54E-09	69133.1
1.1E-08	16340.95	4640.46	9.85E-09	55510.8
1.331E-08	0.00	0.00	1.02E-08	41578.9
1.5E-08	3880.52	1827.56	1.05E-08	29814.2
1.7E-08	12828.34	7177.44	1.11E-08	17430.3
2E-08	25567.12	17315.82	1.17E-08	8761.61
2.2E-08	31878.74	23701.11	1.33E-08	0
2.4E-08	36488.60	29166.93	1.58E-08	6284.83
2.6E-08	39745.69	33597.11	1.85E-08	19287.9
2.8E-08	42001.95	37057.21	2.18E-08	31362.2
3E-08	43545.86	39689.36	2.57E-08	40340.6
3.2E-08	44594.09	41653.32	2.91E-08	44055.7
3.4E-08	45302.17	43097.55	3.31E-08	46222.9
3.6E-08	45778.90	44147.79	3.75E-08	47151.7
3.8E-08	46099.17	44904.88	4.09E-08	47461.3
4.4E-08	46554.41	46106.14	4.46E-08	47770.9
4.6E-08	46618.96	46299.15	4.74E-08	48080.5

Table 3: Theorttical and experimental Values of potential energy for exited state $A^1\Pi$ of BeO molecule.

| r (cm)	V(r) A1Π (cm^{-1}) Morse	V(r) A1Π (cm^{-1}) Varshni	r (cm) [3]	V(r) A1Π (cm^{-1}) experimental [3]
8E-09	177438.29	27569.71	9.23E-09	91114.6
9E-09	108761.18	23332.07	9.54E-09	74086.7
1E-08	64757.96	19087.74	1.08E-08	46842.1
1.1E-08	37563.81	15370.57	1.20E-08	25479.9
1.33E-08	11854.32	10146.81	1.28E-08	14644
1.46E-08	9406.62	9459.06	1.46E-08	9690.4
1.7E-08	13666.75	11333.05	1.97E-08	25479.9
2E-08	23304.76	17286.87	2.54E-08	41269.3
2.2E-08	29206.08	22004.93	2.89E-08	47151.7
2.4E-08	34045.03	26615.85	3.22E-08	50557.3
2.6E-08	37814.35	30798.59	3.68E-08	53034.1
2.8E-08	40662.95	34410.72	4.09E-08	53962.8
3E-08	42775.14	37423.83	4.46E-08	54582
3.2E-08	44321.86	39874.15	4.82E-08	55201.2
3.4E-08	45445.03	41828.89	4.95E-08	55510.8
3.6E-08	46255.96	43365.33		
3.8E-08	46839.12	44559.01		
4.4E-08	47770.59	46712.91		
4.6E-08	47923.36	47115.66		
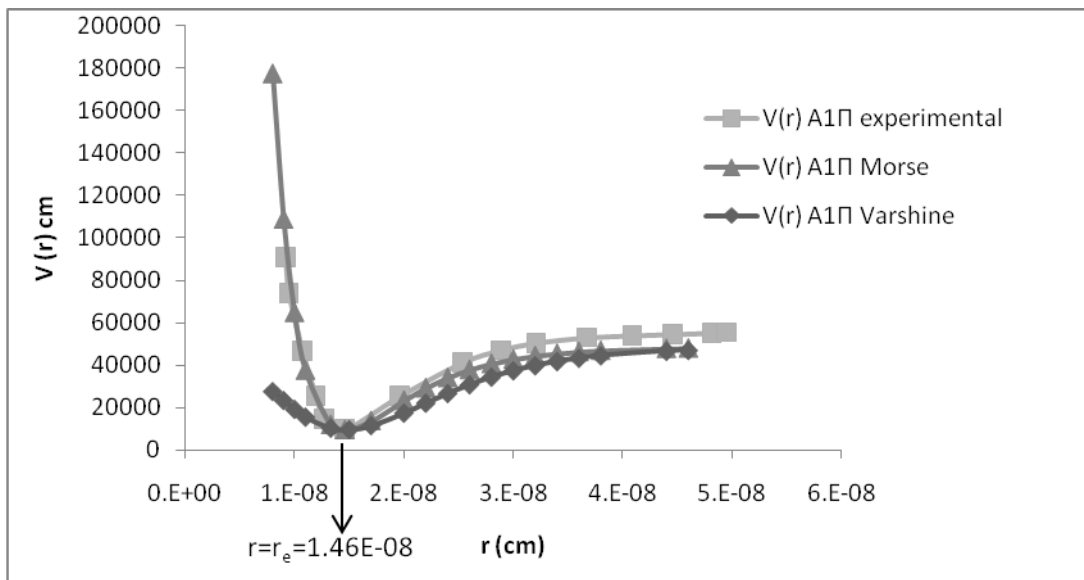
Fig.2: Theoretical potential calculated by Morse and Varshine function compare with the experimental curves for exited state $A^1\Pi$.

Table 4: Theoretical and experimental values of potential energy for exited states $B^1\Sigma^+$ of BeO molecule.

r (cm)	V(r) $B^1\Sigma^+$ (cm^{-1}) Morse	V(r) $B^1\Sigma^+$ (cm^{-1}) Varshine	r (cm) [3]	V(r) $B^1\Sigma^+$ (cm^1) experimental [3]
8E-09	156882.50	34409.54	9.08E-09	111858
9E-09	97426.22	31022.86	9.23E-09	103808
1E-08	60286.56	27590.31	9.69E-09	82755.4
1.2E-08	26770.91	22560.74	1.02E-08	64798.8
1.4E-08	21471.98	21322.95	1.05E-08	51176.5
1.6E-08	27506.64	23739.73	1.12E-08	37244.6
1.8E-08	37008.78	28768.44	1.22E-08	26718.3
2E-08	46554.37	35227.52	1.37E-08	22074.3
2.2E-08	54847.81	42144.06	1.68E-08	30123.8
2.4E-08	61567.41	48848.17	1.82E-08	37554.2
2.6E-08	66801.15	54947.00	1.98E-08	44984.5
2.8E-08	70779.64	60257.58	2.14E-08	52414.9
3E-08	73756.56	64737.24	2.40E-08	62322
3.2E-08	75960.57	68427.07	2.60E-08	66965.9
3.4E-08	77580.52	71411.22	2.89E-08	72229.1

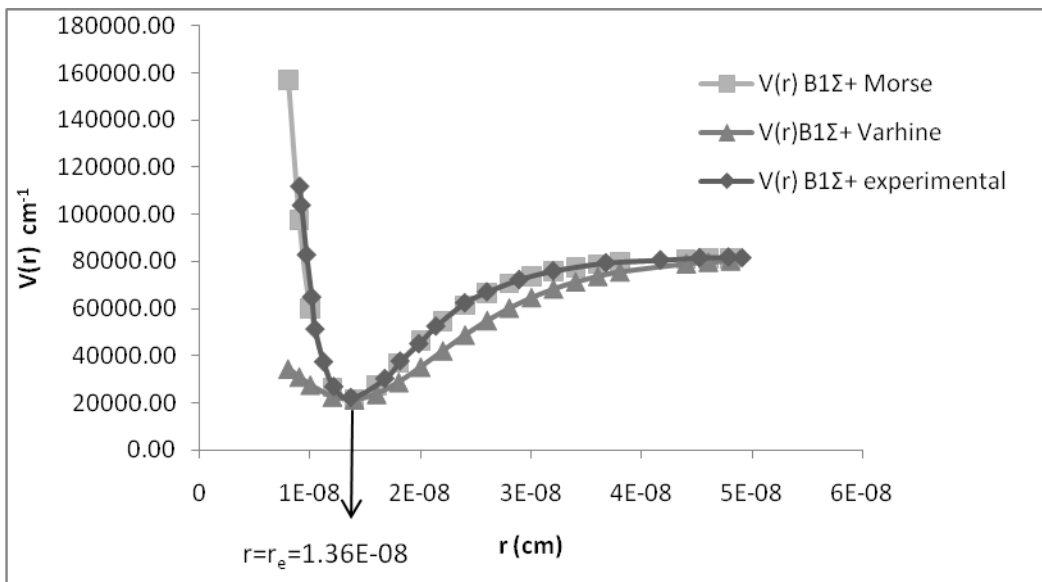| r (cm)	V(r) $B^1\Sigma^+$ (cm^{-1}) Morse	V(r) $B^1\Sigma^+$ (cm^{-1}) Varshine	r (cm) [3]	V(r) $B^1\Sigma^+$ (cm^1) experimental [3]
3.6E-08	78765.18	73790.34	3.20E-08	75944.3
3.8E-08	79628.43	75665.63	3.68E-08	79349.8
4.4E-08	81040.99	79140.68	4.17E-08	80588.2
4.6E-08	81279.80	79811.35	4.52E-08	81517
4.8E-08	81452.56	80323.27	4.78E-08	81826.6
			4.91E-08	81517

Fig.3: Theoretical potential calculated by Morse and Varshine function compare with the experimental curves for exited state $B^1\Sigma^+$.

Fortrat parabola has been calculated by using eq. (10 and 11) as show in Tables (5 and 4). In the electronic transition A1Π-$X^1\Sigma^+$ shows in Fig. 4. When $Bv' < Bv''$ as the length of the band in the lower lectronic state is less than the length of band in the upper electronic state of the world as that Bv change inversely with the square along the band, as show in Fig. 5. So the value of the quantity $Bv' - Bv''$ in eq. (10 and 11) is negative. It appears that the spectra lines values R(J) at m= J+1 increase at first, then decrease because the third term in the right side of eq. (10 and 11) becomes larger than the second term, therefore, we find that R(J) values deviate forming Fortrat parabola and extreme curving representing the band head

towards red region. As regards the spectra lines values P(J) at m= -J and Q(J) at m= J, they decrease when increasing m values. In this case the band head lies in the R branch. In the transition $B^1\Sigma^+$- $A^1\Pi$ shows in Fig. 4. When $Bv' > Bv''$ the length of the band in the upper electronic state less than the length of the band in the electronic, as show in Fig.6. so the value of the quantity $Bv' - Bv''$ in eq. (10 and 11) is positive. It appears that the spectra lines values P(J) at m= -J decrease at first, then increase because the third term in the right side of eq. (10 and 11) becomes larger than the second term, therefore, we find that P(J) values deviate forming Fortrat parabola and extreme curving representing the band head towards

violet region. As regards the spectra lines values R(J) at m= J+1 and Q(J) at   m= J, they increase when increasing m values. In this case the band head lies in the P branch. (We take absolute values of m).

where $X^1\Sigma^+$ represent the electronic ground state, $A^1\Pi$ represent the electronic first excited state and $B^1\Sigma^+$ represent the electronic Second excited state.
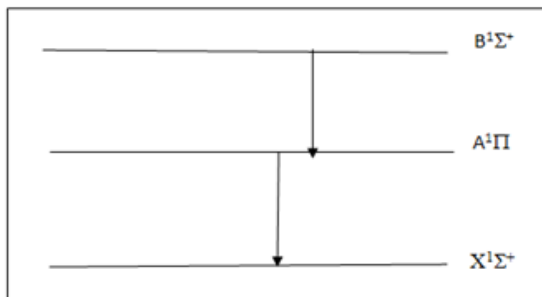

Fig.4: Diagram for electronic transition between molecular energy levels.

Table 5: Values of wave numbers for P,Q and R branch for $A^1\Pi$-$X^1\Sigma^+$ system.

| J	$\overline{v}_{P(J)}$ cm^{-1}	$\lvert$ m-P $\rvert$	vQ(J) cm-1	m-Q	$\overline{v}_{R(J)}$ cm^{-1}	m-R
1	9231.64	-1	9234.39	1	9239.89	2
2	9227.82	-2	9233.32	2	9241.57	3
3	9223.47	-3	9231.72	3	9242.71	4
4	9218.58	-4	9229.58	4	9243.32	5
5	9213.16	-5	9226.91	5	9243.40	6
6	9207.21	-6	9223.70	6	9242.94	7
7	9200.72	-7	9219.96	7	9241.95	8
8	9193.69	-8	9215.68	8	9240.42	9
9	9186.13	-9	9210.87	9	9238.36	10
10	9178.04	-10	9205.53	10	9235.76	11
11	9169.41	-11	9199.65	11	9232.63	12
12	9160.25	-12	9193.23	12	9228.96	13
13	9150.55	-13	9186.28	13	9224.76	14
14	9140.32	-14	9178.80	14	9220.03	15
15	9129.55	-15	9170.78	15	9214.76	16
16	9118.25	-16	9162.23	16	9208.95	17
17	9106.42	-17	9153.14	17	9202.61	18
18	9094.05	-18	9143.52	18	9195.74	19
19	9081.14	-19	9133.36	19	9188.33	20
20	9067.70	-20	9122.67	20	9180.39	21
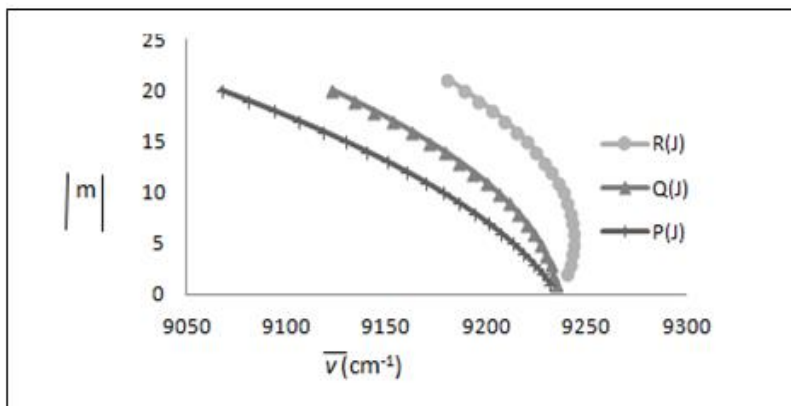
Fig.5: Fortrat parabola of BeO molecule for $A^1\Pi$-$X^1\Sigma^+$system.

Table 6: Values of wave numbers for P,Q and R branch for $B^1\Sigma^+$- $A^1\Pi$ system.

| J	$\overline{\nu}_{P(J)}$ cm^{-1}	$|$ m-P$|$	$\nu_{\overline{Q(J)}}$ cm^{-1}	m-Q	$\overline{\nu}_{R(J)}$ cm^{-1}	m-R
1	11959.07	-1	11962.24	1	11968.57	2
2	11956.81	-2	11963.14	2	11972.64	3
3	11954.99	-3	11964.49	3	11977.16	4
4	11953.63	-4	11966.30	4	11982.13	5
5	11952.72	-5	11968.55	5	11987.56	6
6	11952.26	-6	11971.26	6	11993.43	7
7	11952.25	-7	11974.42	7	11999.75	8
8	11952.69	-8	11978.03	8	12006.53	9
9	11953.58	-9	11982.09	9	12013.76	10
10	11954.93	-10	11986.60	10	12021.43	11
11	11956.72	-11	11991.56	11	12029.56	12
12	11958.97	-12	11996.97	12	12038.14	13
13	11961.66	-13	12002.84	13	12047.17	14
14	11964.81	-14	12009.15	14	12056.66	15
15	11968.41	-15	12015.92	15	12066.59	16
16	11972.46	-16	12023.13	16	12076.97	17
17	11976.96	-17	12030.80	17	12087.81	18
18	11981.92	-18	12038.92	18	12099.09	19
19	11987.32	-19	12047.49	19	12110.83	20
20	11993.17	-20	12056.51	20	12123.02	21
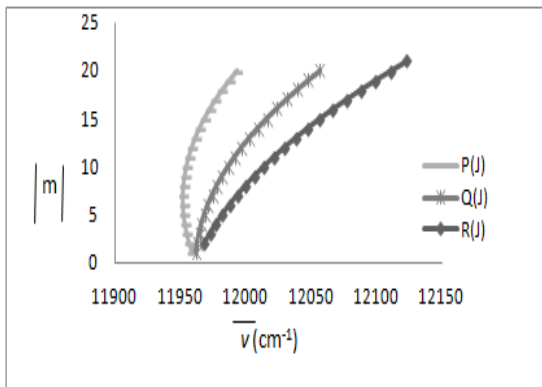
Fig.6: Fortrat parabola of BeO molecule for $B^1\Sigma^+$- $A^1\Pi$ system.

Conclusions

1-The potentials energy of BeO molecule by using Morse and Varshni functions are in good agreement with experimental results and the depth of the potential energy curve in ground state $X^1\Sigma^+$ is greater than the excited state for both $A^1\Pi$ and $B^1\Sigma^+$, which indicate that the ground state is more stable.

2- Fortrat parabola for $A^1\Pi$-$X^1\Sigma^+$ system the band head lies in R(J) and the bands degraded to red region because $Bv' < Bv''$.

3-Fortrat parabola for $B^1\Sigma^+$- $A^1\Pi$ system the band of head lies P(J) the bands degraded to violet region because $Bv' > Bv''$.

References

[1] R. Ropp, Encyclopedia of the Alkaline earth compounds, Elsevier, London, (2012) 106-107.

[2] N. Tawde and V. Tulasigeri, Acta Physica Hungarica, 60 (1986) 113.

[3] A. Lagerqvist, P.hD. Thesis, Faculty of Mathematics and Natural Science, University of Stockholm, Stockholm (1948) 85.

[4] G. Herzberg, Molecules Spectra and Molecules Structure Spectra of Diatomic Molecules, Van Nostrand, New York (1950) 260.

[5] J. Conkic, J. Janjic, D. Pesic, D. Rakotaorijmy, B. Vujisc, and S. Weniger: J. Astrophysical (1978) 1164.

[6] B. Narasimhamurthy, N. Rajamanickam, J. Astrophys. Astr. 4 (1983) 57.

[7] H. Lto, Y. Ozaki, K. Suzuki, T. Kandow, and K.Kuchistu: J.Chem. Phys., 96 (1992) 4196.

[8] T. Hiroa, T. Pinchemel, B. and P Bernath, J. Mol. Spectr., 202 (2000) 216.

[9] J. Daily and M. Branch: J. Mol. Spectr. 214 (2002) 111.

[10] D. Groh, R. pandey, M. Sahariah, E. Amzallag, I. Baraille, M. Rerat, J. Phys. Chem. Solids, 70 (2009) 789.

[11] D. Amiedy , Z. Saleh and R. Yasari, Giorgio. Ronchi, LXV11, 6 (2011) 822.

[12] A. Shayesth, R. Ram and P. Bernath, J. Mol. Spectr, 288 (2013) 47.

[13] J. Graybel, Molecular Spectroscopy, MC Graw Hill Company, New York (1988) 136.

[14] G. King, Spectrascopy and Molecular Structure, Holt, Rinehart and Winston, New York, (1964) 197-199.

[15] D. Sindhu, Fundamentals of Molecular Spectroscopy, Hansraj College, Delhi. p.133-161.

[16] C. Banwell, Fundamentals of Molecular Spectroscopy, Hill Book Company, London (1983) 211.

[17] K. Huber and G. Herzberg, Constants of Diatomic Molecules, Van Nostrand Reinhold, New York (1979) 82.